AIRFOIL DESIGN OPTIMIZATION USING NAVIER-STOKES EQUATIONS AND SIMULATED ANNEALING

S. L. Lee and M. Damodaran
School of Mechanical and Production Engineering, Nanyang Technological University
Nanyang Avenue, SINGAPORE 639798

Abstract

This study is concerned with the application of the basic and a modified simulated annealing algorithm for optimizing aerodynamic objective functions representing transonic airfoil shape optimization problems and which are computed using an explicit finite volume multi-stage and a multi-grid method for solving the compressible Navier-Stokes equations. Airfoil shapes are represented by parametric functions to define the design variables which are altered during the optimization process. Integration of the optimization method, geometric definition and CFD to achieve feasible optimal shapes are demonstrated for the problem of inverse airfoil design and to the problem of maximizing the lift to drag ratio at a given flight condition. The study shows that the proposed approach is feasible in obtaining optimal aerodynamic shape, that the efficiency of the optimization process can be enhanced by modifying the basic simulated annealing and leads to improved designs than could be obtained using deterministic methods.

1 Introduction

Problems concerning the design of transonic airfoil shapes to satisfy desired aerodynamic behaviour can be classified as constrained and unconstrained design optimization problems which require a baseline airfoil configuration to initiate the design process. The optimization of selected aerodynamic parameters such as aerodynamic lift, drag or pitching-moment subject to some imposed design constraints generally belong to the class of constrained optimization problems.   An example of unconstrained design problem is the inverse design method which attempts to solve the inverse problem of determining the airfoil shape that will support a specified (target) airfoil surface pressure distribution i.e. the airfoil shape is determined by minimizing the discrepancy between the target and the evolving airfoil surface pressure distribution. Advances in computational fluid dynamics (CFD) techniques for solving the Navier-Stokes equations of viscous compressible fluid motion have strong implications for their use in evaluating objective functions which are to be optimized in the computational design environment. One significant implication is the coupling of these techniques with appropriate numerical optimization algorithms to develop efficient and robust computational methods for the optimum design of fluid machinery and aerodynamic components as outlined in Labrujere and Sloof [1].

The present study is focused on the application of basic and modified simulated annealing (SA), a stochastic optimization method for inverse and constrained aerodynamic design of transonic airfoil shapes in which a compressible Navier-Stokes flow solver is used to evaluate the objective function. SA as outlined in Kirkpatrick et al [2] and in Corona et al [3] is a stochastic global optimization method which has proven to be a good tool for complex nonlinear optimization problems and has been applied to a variety of problems. Aly et al [4] has applied it for the design of optimal aerodynamic shape of axisymmetric forebody for minimum drag where SA is used as the outer optimization loop and calls the flow solver to evaluate the objective function. SA has the advantage of yielding a global minimum and in overcoming the limitations of deterministic gradient-based search methods such as in Eyi and Lee[5] which have a tendency of getting trapped in local minima.

2 Formulation

2.1 Parametric Representation of Airfoil Shape and Definition of Design Variables

The design process is initiated by defining design variables controlling the airfoil shape. This is achieved by an approximate representation of the airfoil shape which will evolve during the design cycle. In order to maintain control over the size of the design space, a baseline airfoil is first chosen and the steady flow field around it for a specific Mach number and angle of attack is computed for starting the design cycle iterations. The airfoil shape is updated by adding a smooth perturbations $\Delta y_k(x)$ defined as a linear combination of a family of smooth curves over the range $0 < x < 1$ as follows:

$$\Delta y_k(x) = \sum_{k=1}^{K} \delta_k f_k(x) \qquad (1)$$

where x is the normalized chord-wise position of the coordinates defining the airfoil contour, δ_k are the design variables which will change during the design iterations and K is the number of basis functions $f_k(x)$, one form of which is defined in Hicks and Henne[6] as follows:

$$f_1(x) = x^{0.25}(1-x)^{-20x} \; ;$$
$$f_k(x) = sin^3(\pi x^{t(k)}) \; k>1; \; 0<x<1 \qquad (2)$$

where $t(k) = (log\,0.5)/(log\,x_k)$ and x_k represents the location of the maximum values of $f_k(x)$. When these functions are distributed over the entire airfoil chord on both the upper and lower surfaces, they admit a large possible design space. Other basis functions such as Wagner functions outlined in Ramamoorthy and Padmavathi [7] can also be used in place of Hicks-Henne functions to represent the airfoil shape and to restrict the design space.

For inverse design problems a typical objective function $J(X)$ to be minimized is defined as follows:

$$J(X) = \left(\frac{\sum_{m=1}^{M}(P_{t_m}-P_{b_m})^2 \Delta S_m}{\sum_{m=1}^{M} \Delta S_m} \right)^{1/2} \qquad (3.1)$$

where P_{t_m} is the pressure distribution of the target airfoil that we are seeking, P_{b_m} is the pressure distribution of the designed airfoil which evolves after each design iteration, ΔS_m is the length of the airfoil surface element and the summation is done for the M coordinate points defining the airfoil contour. For constrained aerodynamic design problems such as the minimization of drag the objective functions such as drag coefficient are evaluated by the flow solver for each design iteration along with additional constraints which are handled by way of penalty functions to augment the constraints with the objective function to create a modified objective function which is optimized so that the additional terms associated with the constraints will vanish as soon as global minima is reached or by eliminating infeasible designs by appropriate barrier functions. This class of design optimization problems is known as direct numerical optimization or design by optimization and generally has a higher level of automation than that for inverse design. A typical constrained design problem is to obtain an airfoil shape which produces maximum aerodynamic efficiency, i.e. the ratio of aerodynamic lift (L) over drag (D) at a specified flight condition while maintaining the lift at the original level. As this a design problem that maximizes its objective function, it is necessary to reverse the sign of the objective function in the minimization algorithm used in the inverse design. The aerodynamic drag, lift and efficiency are computed using the Navier-Stokes CFD solver for each iterated design shape. Two inequality constraints are imposed on the design process to ensure that the aerodynamic lift and cross-sections area of the airfoil do not decrease during the optimization process. In mathematical form the problem is defined as follows:
:
Maximize:

$$J(X) = C_l / C_d \qquad (3.2)$$

Subject to:

$$g_1(X) = 1 - \frac{C_l}{C_{l_0}} \le 0 \; , \; g_2(X) = 1 - \frac{A}{A_0} \le 0$$

where X is the vector of k design variables δ_k, C_l and C_d are the aerodynamic lift and drag coefficients respectively, A is the airfoil area, A_0 is the area of the baseline airfoil and C_{l0} denotes the initial value of the lift coefficient which has to be maintained.

2.2 CFD Analysis for Evaluating Objective Function

The flow analysis module used to evaluate the objective function is based on the finite volume formulation of the unsteady Navier-Stokes equations for two-dimensional viscous flow. In Cartesian coordinate system, the integral form for a region A with a bounded surface B takes the form:

$$\frac{\partial}{\partial t} \iint_A \mathrm{w}\, dx dy + \int_B F_c \bullet ds = \int_B F_v \bullet ds \qquad (4)$$

where $F_c = f\vec{i} + g\vec{j}$ and $F_v = F\vec{i} + G\vec{j}$, $\mathbf{w}$ is the vector of the conservative dependent variables, $\mathbf{f}$ and $\mathbf{g}$ and are the convective flux vectors, $\mathbf{F}$ and $\mathbf{G}$ are the viscous flux vectors and these are functions of p, ρ, u, v, w, E and T which are the pressure, density, cartesian x- and y- velocity components, and specific total energy and local temperature. The pressure is obtained from the equation of state for a perfect gas. A structured grid is used to discretize the physical domain into a large number of quadrilateral cells whose cell centers are labelled by the subscript indices (i,j) along the ξ and η coordinate directions. The application of the integral law of Eq.(4) separately to each cell results in a system of ordinary differential equations of the form

$$\frac{d}{dt}(hw)_{i,j} + Q_{i,j} - D_{i,j} = 0 \qquad (5)$$

where $h_{i,j}$ is the area of the quadrilateral cell, $Q_{i,j}$ is the estimate of the net convective and viscous flux out of the boundaries of the cell and $D_{i,j}$ is the adaptive artificial dissipation terms which is a blend of second and fourth differences in the flow variables and which are explicitly added for shock capturing and numerical stability purposes. The equations are advanced from a set of initial conditions to steady state solutions for the desired flow conditions by a multi-stage time-stepping scheme. Several convergence acceleration strategies such as local time-stepping, implicit residual smoothing and multi-grid strategies are used to accelerate the computation of steady state solutions. Characteristic boundary conditions are imposed at the far-field boundaries while no-slip condition is imposed on the airfoil surface which is also assumed to be adiabatic. A simple algebraic turbulence model is used to address the turbulence closure The readers can refer to and Jameson and co-workers [8-9] and Damodaran and Lee[10] for specific details of the flow modeling outlined above.

2.3 Design Optimization using Simulated Annealing (SA)

The minimization of this objective function could be accomplished by either deterministic gradient-based methods or stochastic methods. In this work traditional SA as well as a modified version of it is applied to seek optimum aerodynamic shape designs for both inverse design as well as constrained design problems in the transonic flow regime. SA is analogous to the physical process of annealing of solids by cooling molten solids from a high temperature to a lower temperature according to a cooling schedule. The analogy is used because solids cooled sufficiently slowly attain a state of minimum energy. This is a concise optimization algorithm which is based on Monte-Carlo techniques and starts with a high temperature corresponding to the cycle N=1. The objective function is calculated based on an initial (baseline) configuration (defined by a the initial state of the vector of design variables which define the baseline airfoil shape) and this is followed by the random generation of a new configurations (new vectors of design variables). New trial points are generated around the current design vector by applying random moves along each design coordinate. The new design coordinate values are uniformly distributed in intervals centered around the corresponding coordinate and a step vector is used to guide the extent of the random moves. The step vector V_M is adjusted periodically through the step adjustment vector H, N_T times to adapt to the behaviour of the objective function. The new

configuration is accepted as the current configuration if this change in the objective function is less than or equal to zero or if the change is greater than zero provided the change in objective function also satisfies the Metropolis criterion which measures the acceptance probability. The random generation of new design vectors and the satisfaction of the acceptance criteria is repeated for N_s times till the Markov chain is completed at a given temperature. Then the temperature is lowered via temperature reduction factor R_T and a new sequence of moves generated and the cycle is repeated till the design vector converges to the optimum value. The basic simulated algorithm consists of several tuning parameters which can be adjusted to improve the performance of the optimization method. One drawback of the traditional simulated annealing method is that it has a fixed cooling schedule which does not take into consideration the stage the algorithm is in. It may be better to use a faster or a slower cooling rate at a particular stage. To incorporate a degree of adaptiveness into the method it is possible to regulate the cooling schedule by introducing a new parameter T_c which depends on the ratio of accepted moves R_{CA} to the total number of moves after $N_s x N_T x N$ cycles and by setting a range by user specified values of $R_{c,high}$ and $R_{c,low}$ which are respectively the upper and lower bounds on this ratio to define the parameter which can be used to reduce the temperature. If R_{AR} (ratio of accepted to rejected moves)$<R_{c,low}$, the cooling rate is reduced, otherwise the cooling rate is kept the same. If $R_{AR} > R_{c,high}$ the cooling rate is increased otherwise it is kept the same. The additional tuning parameters can be manipulated to boost the efficiency of the traditional simulated annealing algorithm and the degree of the boost depends on the problem being addressed. Details of the tuning parameters of SA and SACAR are outlined in Lee [11].

3 Results and Discussions

Computational results are presented and discussed for the problems of inverse design of transonic airfoils and the constrained design problem of transonic airfoil lift/drag (L/D) maximization. The flow field and objective functions are computed on a body conforming C-grid around the airfoil consisting of 128x48 cells (coarse grid) and 256x64 cells (fine grid). The airfoil shape is parameterized using 14 basis functions- seven of which are used to define the upper surface of the airfoil and the remaining 7 to define the lower surface of the airfoil. This representation gives rise to 14 design variables for the parametric representation of the airfoil shape which are varied during the steps of the design cycle so as to estimate the perturbations in the design variables which will minimize the objective function defined by Eqn (3.1) and which enables the modification of the airfoil contour as well as the computational grid. CFD analysis is used to calculate the airfoil surface pressure distribution for the baseline airfoil shape as well as each subsequent shape of the designed airfoil. During each design cycle the flow solution corresponding to the previous design flow analysis is used as initial conditions so as to reduce computational time for evaluating the objective function using CFD. Where possible comparisons will be made with results obtained for selected transonic airfoil design problems using deterministic methods in Lee and Eyi [12] and Eyi et al [13] for the same problems considered in this paper.

3.1 Inverse Design of Transonic Airfoils

In order to demonstrate the application of stochastic optimization methods for inverse design of transonic airfoils, the target pressure distribution which is the desirable goal of the design is chosen to correspond with the pressure distribution around a RAE 2822 (target airfoil) immersed in transonic flow at a Mach number $M = 0.730$, angle of attack $\alpha = 2.78°$ and Reynolds Number $R_e = 6.5 \times 10^6$. In order to initiate the design process to seek the airfoil shape which will correspond to the target pressure distribution an initial guess for the airfoil shape has to be made and this initial shape (baseline airfoil) is chosen to correspond to the NACA-0012 airfoil at the same flow conditions. Since the target pressure distribution has been defined to correspond to that of a well known airfoil shape i.e. RAE 2822, the quality of the final design shape achieved by the optimization process can be compared to the shape of the RAE 2822 to

make an assessment on the robustness, accuracy and effectiveness of the optimization scheme. The optimization process employed stringent terminating criteria in order to achieve a fully optimized design. For the calculations shown in this section, all SA runs terminate if 4 successive local optimum obtained after 4 temperature reductions differ by less than a specified tolerance, i.e. 10^{-4}. In general one could specify different tolerance limits that are more stringent than this value but it will be at the expense of higher computational costs. Numerous design optimization runs using SA have been attempted with different sets of values for the SA tuning parameters. The values of the SA tuning parameters employed for this investigation are $R_T=0.1$ $V_M=0.001$, $H=2.0$, $N_S=10$, $N_T=5$.The value of the objective function based on the baseline airfoil is 0.11420. Figure 1.1 shows the variation of the value of the objective function from the initial value to the final optimized value by the SA algorithm.
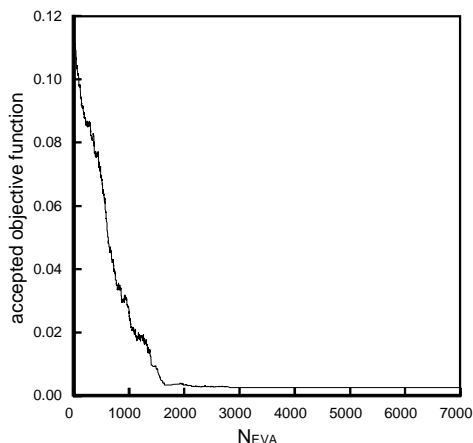
Fig 1.1 Objective function Convergence (SA)

The objective function reduced to a value of 0.00249 during the minimization process by SA. The number of function evaluations (N_{EVA}) to achieve this reduction is about 7000. The geometric shape and surface pressure coefficient distribution of the baseline airfoil, the target airfoil and the designed airfoil are compared in Figures 1.2 and 1.3.
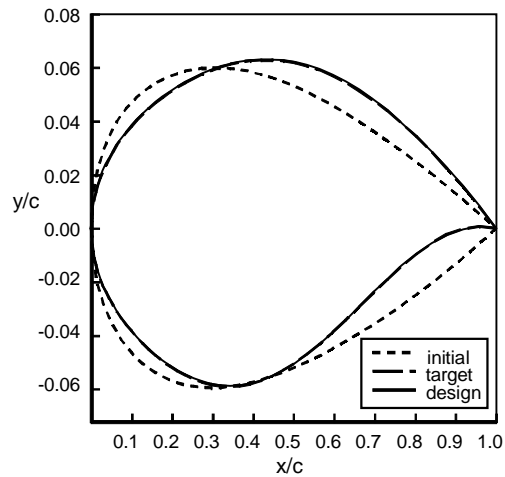
Fig 1.2 Initial, design and target airfoil shapes
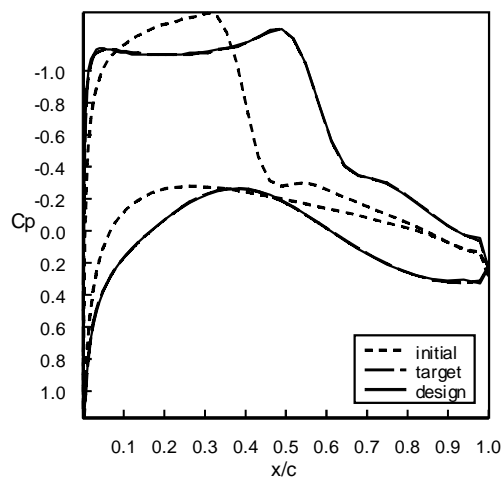
Fig 1.3 Initial, design and target airfoil surface pressure coefficient distributions

Figures 1.4 and 1.5 show the variation of the 14 design variables and their corresponding step length parameter with the number of function evaluations.

It can be seen from these figures that the steepest drop in the objective function occurs during the first 2000 iterations beyond which the rate of decrease of the objective function becomes marginal. The intermittent increases in objective function during the first 2000 iterations are due to the fact that SA randomly allows the degradation of solution to avoid getting trapped in local minima.
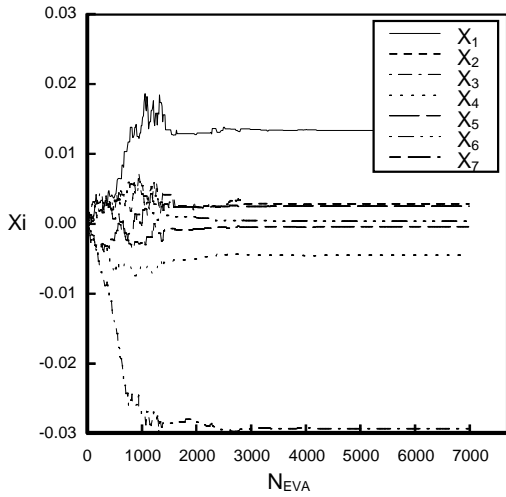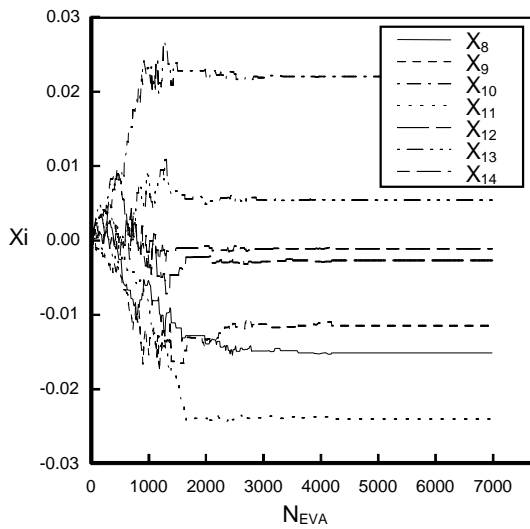
Fig 1.4 Convergence of the 14 design variables

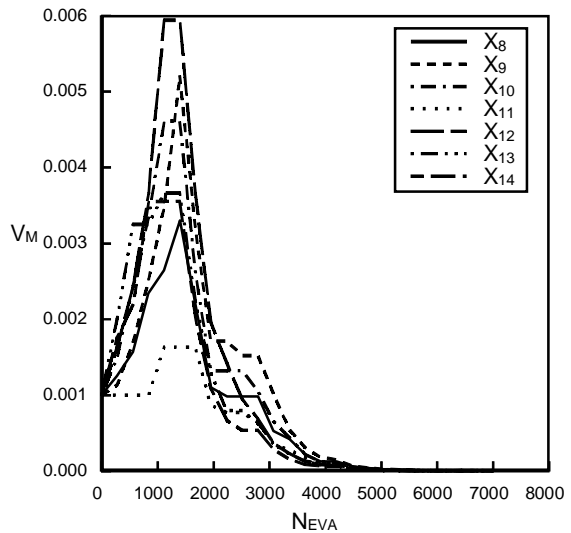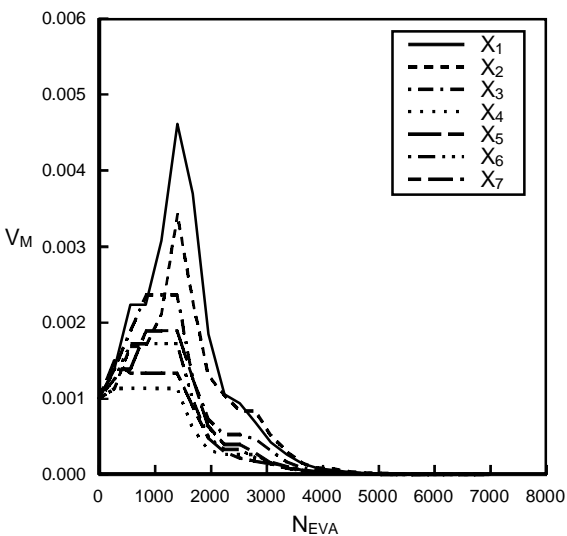**Fig 1.4 Convergence of the 14 design variables (Continued)**

Fig 1.5 Variation of V_m for the 14 design variables

Since the probability of such random degradation depends on the annealing temperature as well as the magnitude of degradation, most of these degradations tend to occur in the initial stage of the optimization process i.e. first 2000 iterations. As the temperature drops further, a decrease in the number of occurrences of degradation as well as the magnitude of degradation allowed is observed. This accounts for the relatively flat portion of the convergence curve after 2000 iterations.

Figure 1.4 shows no large oscillatory behavior. This suggests that the initial step length is sufficiently small. It can also be seen that most of the variation in the value of the design variables occurs during the first 4000 iterations with the most significant variations occurring during the first 2000 iterations. This observation correlates with the observation made from the convergence history of the objective function. Fig. 1.5 shows that the step length increases sharply from the initial value for the first 1800 iterations before decreasing sharply. The sharp increase corresponds with the significant changes in the objective function whereby most of the trial solutions are accepted i.e. acceptance ratio is greater than 0.5. Subsequent decrease in step length indicates that the acceptance ratio drops below 0.5 as the optimization process approaches the global minimum. It can also be seen that the variation of the design variables for the lower airfoil surface are larger than those of upper airfoil surface. The evolving airfoil shape

requires a careful grid adjustment so as to facilitate the flow calculation using CFD analysis.

3.2 Maximization of Airfoil L/D Ratio

The application of SA to the problem of transonic airfoil aerodynamic efficiency maximization is considered next. The test case chosen is that of transonic flow past a RAE2822 airfoil at Mach number 0.730 and angle of attack 2.46^{o}. The Reynolds number is 6.5×10^{6}. This is an example in which constraints are applied. Constraints have been handled by using barrier functions and also by way of augmenting the constraints with the objective function with penalty functions. The change in the order of magnitude of the objective function requires a corresponding adjustment in the initial annealing temperature T_{o} in order to maintain the same order of magnitude of the Metropolis criteria computation that will provide flexibility in overcoming local optima and searching for global optimum. The values of the SA tuning parameters employed for this investigation are $R_{T}=0.1$ $V_{M}=0.001$, H=1.0, $N_{S}=20$, $N_{T}=5$.All computations terminate when the successive local optima obtained after four temperature reductions differ by less than a specified tolerance, i.e. 1×10^{-8}.

The initial value of C_{l}/C_{d} obtained using CFD analysis was 36.448.The final design value obtained from this optimization process and CFD analysis was 45.549.The change in lift coefficient was much less than 1% while the change in the drag coefficient was around 20%. The computed results show that the airfoil designs obtained from the SA algorithm yield an increase in C_{l}/C_{d} by about 30 % while having marginal increases (less than 1 %) in both C_{l} and area. It can be seen that the increase in C_{l}/C_{d} is mainly due to the significant reduction in the aerodynamic drag and the increase in the aerodynamic lift are marginal in view of the imposed constrained.

Fig. 2.1 shows the variation of the value of the objective function from the initial value to the final optimized value as the objective function increased by SA vs. the number of function evaluations (NEVA). The figure shows that the variation flattens beyond the value of

NEVA = 1000, indicating that the global optimum has been obtained.
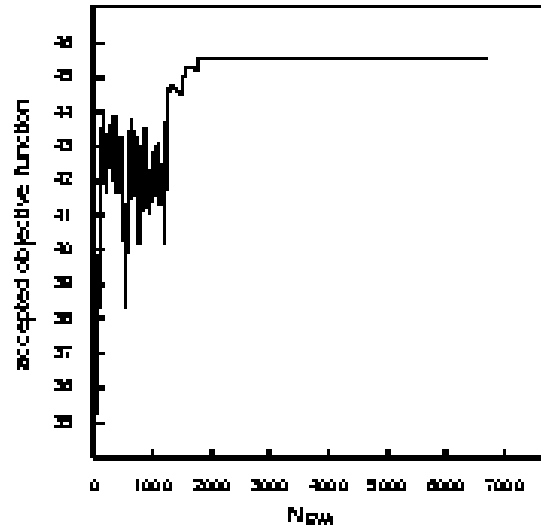
Fig 2.1: Convergence of Objective Function

A comparison of the geometric shape of the baseline airfoil which is the standard RAE 2822 airfoil used as the initial guess for the optimization process and the designed airfoil is shown in Figure 2.2.
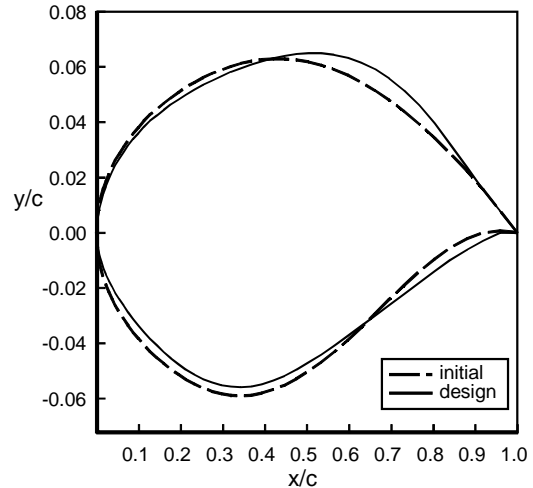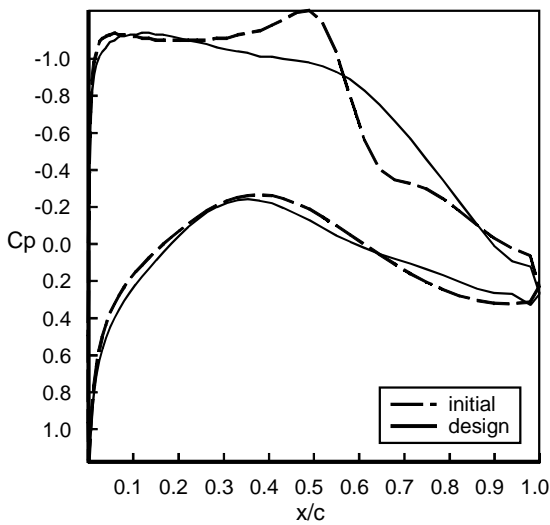

Fig 2.2 : Airfoil Shape: Baseline vs Designed

The comparison of the airfoil surface pressure coefficient distribution corresponding to the baseline airfoil and the designed airfoil is shown in Fig 2.3.

It can be seen from these figures that the drag reduction that contributed to the increase in aerodynamic efficiency is achieved by altering the airfoil shape to weaken the strong shock wave on the upper surface of the baseline airfoil.

The weakening of shock waves on the surface of airfoil generally reduced the wave drag and gives rise to an overall aerodynamic efficiency.
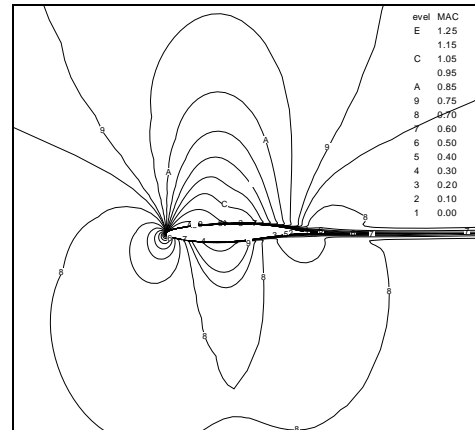

Fig 2.3 : Distribution of Airfoil Surface Pressure Coefficient: Baseline vs Designed

Fig. 2.4 shows the contours of local Mach number in the vicinity of the initial or baseline airfoil.
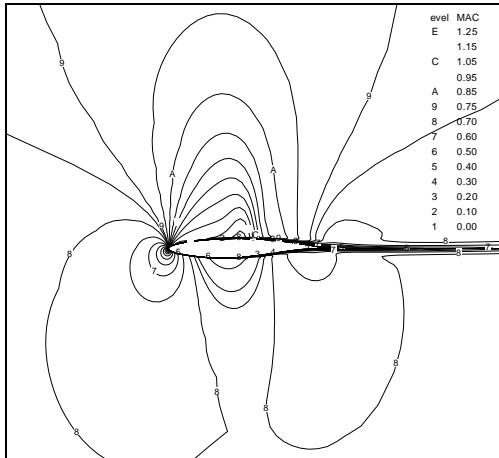

**Fig 2.4: Mach Number Contours corresponding to baseline airfoil**

Fig 2.5: Mach Number Contours coresponding to designed airfoil

By comparing this with the contours of local Mach number in the vicinity of the designed RAE 2822 airfoil as shown in Fig. 2.5, the diffused shock wave on the upper surface of the designed airfoil can be seen as the contributing factor to reduced drag and increased efficiency while maintaining the same lift coefficient.

Fig. 2.6 shows the variation of the step length V_m which exhibits a sharp rise during the initial stages of the optimization before decreasing rapidly. Fig. 2.7 shows the variation of two design variables (For sake of clarity, only two design variables that exhibit large variations are presented) which are used for the parametric representation of the airfoil using Hicks-Henne functions with the number of function evaluations (NEVA). From the convergence history of the objective functions, the convergence history of the design variables and the variation in the step length, it can be seen that the objective function exhibits large fluctuations before settling down early in the optimization process. The optimum airfoil contour is obtained after about 2000 iterations which have resulted in greater fluctuations in the value of the objective function and a greater disparity with respect to the initial RAE 2822 airfoil.
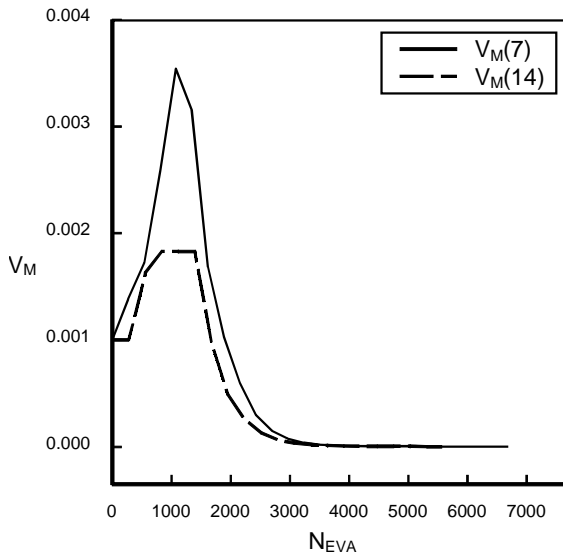
Fig 2.6: Variation of step-length V_m
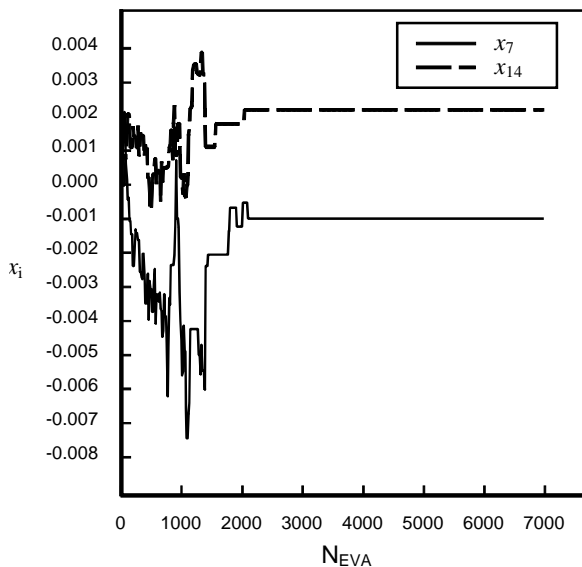
**Fig
2.7: Convergence of Selected Design Variables during
the Optimization Process**

4 Conclusions

In this study the feasibility of applying global stochastic optimization methods such as simulated annealing to both inverse design of airfoil and the constrained design problem of aerodynamic efficiency maximisation has been successfully demonstrated. The use of Navier-Stokes equations improves the level of confidence in the design results as compared to simpler flow models used by earlier researchers. It has also been found that by using global optimization methods it is possible to obtain optimum configurations better than optimal solutions obtained by deterministic methods. As

demonstrated, with the continuous advances in computational capability, the stochastic optimisation is affordable even though high-level physics are used.

References

[1] Labrujere, Th. E. and Sloof, J. W., Annual Reviews in Fluid Mechanics, Vol. 25, pp 183-214,(1993).

[2] Kirkpatrick S., Gelatt C. D. and Vecchi M. P. , Science 220, pp 671-680, (1983)

[3] Corona, M., Marchesi, C, Martini and Ridella S., ACM Transactions on Mathematical Software, Vol 13, No.3, pp.262-280, (1987)

[4] Aly S., Ogot, M. and Pelz R., "Stochastic Approach to Optimal Aerodynamic Shape Design,"AIAA Journal of Aircraft, Vol. 11, No.5, (1996)

[5] Lee, K. D. and Eyi, S., "Airfoil Design Optimization Using the Navier-Stokes Equations", Journal of Optimization Theory and Applications, Vol. 83, No. 3., pp. 447-461, December 1994.

[6] Hicks R. M. and Henne P. A.,"Wing Design by Numerical Optimization", AIAA Paper 79-0080,(1979).

[7] Ramamoorthy, P. and Padmavathi, K.,"Airfoil Design by Optimization", Journal of Aircraft, Vol. 14, pp. 219-221, 1977.

[8] Jameson, A., Schmidt, W. and Turkel, E.,"Numerical Solutions of the Euler Equations by Finite-Volume Methods Using Runge-Kutta Time Stepping Schemes", AIAA Paper 81-1259,(1981).

[9] Martinelli, L., Jameson, A. and Grasso, F., A Multi-grid Method for Navier-Stokes Equations", AIAA Paper 86-0208,(1986).

[10] Damodaran, M. and Lee, K. H., "Finite Volume Calculation of Steady Viscous Compressible Flow Past Airfoils", Journal of Institution of Engineers, Singapore, Vol.33, No.5,pp 39-44. (1993).

[11] Lee, S. L., "Aerodynamic Shape Design of Transonic Airfoils Using Stochastic Optimization Methods and Computational Fluid Dynamics", PhD Thesis, School of MPE, Nanyang Technological University, Singapore, March 2000.

[12] Lee, K. D. and Eyi, S., "Transonic Airfoil Design by Constrained Optimization", AIAA Paper 91-3287-CP, pp 677-687, (1991).

[13] Eyi, S., M. Damodaran and Lee, K. D.,"Inverse Design of Transonic Airfoils", Proceedings of 7th Asian Congress of Fluid Mechanics, pp 275-278, (1997).